J. Membrane Biol. 211, 115–126 (2006)
DOI: 10.1007/s00232-006-0010-9

The Journal of
Membrane
Biology



# Expression and Functional Characterization of the Human Ether-à-go-go-Related Gene (*HERG*) $K^+$ Channel Cardiac Splice Variant in *Xenopus laevis* Oocytes

**Ebru Aydar, Christpher Palmer**
Division of Cell and Molecular Biology, Imperial College, London, South Kensington Campus, Sir Alexander Fleming Building, London SW7 2AZ, United Kingdom

Received: 6 February 2006/Revised: 20 June 2006

**Abstract.** HERG $C_{Cardiac}$, a C-terminal splice variant of the human ether-à-go-go-related gene (HERG A), was identified and found to be 100% homologous to $HERG_{USO}$. Real-time polymerase chain reaction data indicated that in the human heart HERG $C_{Cardiac}$ mRNA was expressed eight times more than HERG A, whereas in human ventricular tissue it was expressed six times more than HERG A. A HERG $C_{Cardiac}$-green fluorescence protein (GFP) construct was heterologously expressed in *Xenopus* oocytes. Confocal micrographs revealed that HERG $C_{Cardiac}$ was mainly expressed in the plasma membrane. HERG $C_{Cardiac}$ channel expressed in oocytes produced slower inactivating outward currents and faster deactivating tail currents than those of HERG A channel. Equal amounts of HERG A and HERG $C_{Cardiac}$ cRNA coinjected into oocytes formed intermediate HERG A + HERG $C_{Cardiac}$ heteromultimers, which was reconfirmed by immunoprecipitation experiments with a HERG A N-terminal antibody. These heteromultimers had different inactivation, deactivation and activation kinetics from those of HERG A and HERG $C_{Cardiac}$ channels. HERG A + HERG $C_{Cardiac}$ heteromultimers significantly reduced the model action potential mean amplitude and increased the fast and slow inactivation $\tau$ values of the action potential repolarization phase, suggesting involvement of HERG A and HERG $C_{Cardiac}$ heteromultimers in modulation of the refractory interval.

**Key words:** HERG — *Xenopus laevis* — Oocyte — $K^+$ channel — eag channel — HERG C terminus

*Correspondence to:* Ebru Aydar; email: e.aydar@imperial.ac.uk

## Introduction

The human ether-à-go-go-related gene HERG (HERG A) encodes a $K^+$ channel that is essential for normal repolarization of the cardiac action potential. HERG A was originally cloned from a human hippocampal cDNA library by homology to the *Drosophila* $K^+$ channel gene *eag* (Warmke & Ganetzky, 1994). HERG A, as well as its isoforms, encodes a component of rapidly activating delayed rectifier $K^+$ current, cardiac $I_{Kr}$ (Sanguinetti et al., 1995; Trudeau et al., 1995; Jones et al., 2004), and is critical for the maintenance of normal rhythmicity in the human heart (Curran et al., 1995). HERG A has electrophysiological properties similar, but not identical, to $I_{Kr}$ (Sanguinetti et al., 1995). The time constants of activation and deactivation of HERG A are four to 10 times slower than native $I_{Kr}$ when expressed in guinea pig and mouse cardiac myocytes (Sanguinetti & Jurkiewicz, 1990). These observed differences in $I_{Kr}$ kinetics suggested the existence of HERG isoforms in the human heart (Pond & Nerbonne, 2001).

Two N-terminal isoforms of mouse ERG (MERG 1a and 1b) have been identified and cloned (London et al., 1997). Subsequently, human cardiac isoforms of HERG A were identified (London et al., 1998). The putative isoform HERG B lacks the first 376 amino acids of HERG A and has an alternate 36-amino acid N-terminal end (32/36 identical to those in MERG 1b). Moreover, London et al. (1998) identified a C-terminal isoform of HERG A, HERG C, from a human infant brain expressed sequence tag (EST) library. Northern blot analysis using isoform–specific probes showed that HERG A was expressed at high levels in heart and moderate levels in smooth muscle and brain, HERG B was expressed at low levels in heart and in smooth muscle, HERG C was expressed at high levels in heart and at low levels in

smooth muscle and brain, and HERG BC (isoform with both alternate 5′ and 3′ ends) was expressed at moderate levels in smooth muscle and at low levels in brain (London et al., 1998). Subsequently, HERG smooth muscle isoform (HERG BC) was cloned (Shoeb, Malykhina & Akbarali, 2003). A human cardiac isoform of HERG A (HERG C) was constructed and named $HERG_{USO}$ (Kupershmidt et al., 1998). Expression of $HERG_{USO}$ channels in $Ltk^-$ cells resulted in nonfunctional channels; however, when coexpressed with HERG A, they were shown to coassemble. Kupershmidt et al. (1998) suggested this isoform might possess a cell-trafficking problem in Ltk cells. They related this trafficking problem to the lack of a 104-amino acid sequence after the cyclic nucleotide binding domain. In contrast, $HERG_{USO}$ was demonstrated to be expressed in human jejunum together with HERG and suggested to play a fundamental role in the control of motility patterns in human jejunum through an ability to modulate the electrical behavior of smooth muscle cells (Farrelly et al., 2003). Additionally, HERG C-terminal deletion constructs lacking 104 amino acids formed functional channels when expressed in *Xenopus* oocytes (Aydar & Palmer, 2001). These data later were explained in relation to an endoplasmic reticulum retention sequence in the HERG C terminus (Kupershmidt et al., 2002).

In the present study, we aimed (1) to determine the functional expression of a HERG C-terminal isoform, HERG $C_{Cardiac}$, in *Xenopus laevis* oocytes, which we constructed from a clone obtained from a human infant brain EST library and which is shown to be abundant in human heart; (2) to distinguish the localization of this isoform in *Xenopus* oocytes; (3) to discover whether this variant is molecularly and functionally associated with HERG A; and (4) to determine the importance of this association in relation to regulation of the action potential (AP).

## Materials and Methods

### Plasmid Construction

HERG A was constructed by restriction digest of pGH19-HERG A with *Bgl*II and *Eco*RI and separation of the DNA fragments by DNA gel electrophoresis and purification of the pGH19-HERG fragment using Qiagen (Valencia, CA) spin columns. Subsequently, HERG $C_{Cardiac}$ cDNA plasmid obtained from Image consortium (EST name yg88f08.s1) was also digested with *Bgl*II and *Eco*RI, and the DNA fragment encoding the C-terminal portion of this HERG $C_{Cardiac}$ isoform was ligated into the pGH19-HERG fragment by mixing equimolar amounts in a ligation mixture (Promega, Madison, WI) containing DNA at room temperature overnight. The ligation was transformed into XL1-Blue cells, spread onto LB-Ampicillin plates and incubated at 37°C overnight. The resulting colonies were screened by polymerase chain reaction (PCR) using HERG $C_{Cardiac}$-specific primers (see below), and positive colonies were amplified to create plasmid minipreparations (Qiagen) and subsequently sequenced using pGH19 vector and HERG A-specific primers (see below). A pGH19-HERG $C_{Cardiac}$-GFP construct was prepared by PCR amplification of HERG $C_{Cardiac}$ from the above construct using the following primers: 5′- gggggatccatgccggtgcggaggggccacg-3′ and 5′-ggggaattcctttaaggaagcaaaaagtg-3′ (the latter removed the stop codon from the sequence and added an *Eco*RI site to the 3′ end of the HERG $C_{Cardiac}$ sequence). This PCR fragment was ligated into a pGH19 vector which contained a GFP gene inserted into the *Hind*III/*Eco*RI sites of this vector such that the GFP was fused in frame with the C terminus of HERG $C_{Cardiac}$. The DNA sequence of this construct was confirmed by DNA sequencing.

### Real-Time PCR

HERG mRNA was quantified by real-time PCR. Human total heart and ventricle tissue cDNA was purchased from Biochain (Hayward, CA). Real-time PCR was performed on a DNA Engine Opticon 2 machine (GRI, UK) with Opticon Monitor software. PCR with SYBR® Green PCR Master Mix (Finnzymes, Espoo, Finland) was performed under the following conditions: 95°C for 30 s, 60°C for 15 s and 72°C for 30 s for 40 cycles. The cycles were preceded by heating for 5 min at 95°C, and following cycle completion, the reactions were incubated for 5 min at 72°C. The primers were as follows: HERG A (sense) 5′-tgcaggcagtcccaggtcc-3′, HERG-A (antisense) 5′-agaagtggtcggagaactca-3′ and HERG $C_{Cardiac}$ (antisense) 5′-tgcaggcagtcccaggtcc-3′. Melting curves and agarose gel electrophoresis were performed to verify the specificity of the product. As variations in cDNA quality within the different samples could occur, β-actin was included as an internal control: (sense) 5′-agcctcgcctttgccga-3′, (antisense) 5′-ctggtgcctggggcg-3′. By subtracting the β-actin threshold ($C_t$) value from the HERG $C_t$ value of each sample, the cDNA quality of each sample is taken into account. The relative quantification of the mRNA levels in each individual sample was calculated according to the model of Pfaffl (2001). For each primer set, a standard curve was made and the slope factor calculated. The corresponding real-time PCR efficiency ($E$) of one cycle in the exponential phase was calculated according to the equation $E = 10(-1/\text{slope})$. The relative HERG isoform ratio ($R$) was calculated according to the equation $R = E$ $C_t$ (control - sample), normalized against the highest individual $C_t$ value obtained for five repeats. A mean was calculated from five normalized repeats, and the standard error of the mean was calculated using one-way analysis of variance (ANOVA), with significance expressed as detailed below.

### Antibodies

An antibody specific to the N-terminus of HERG A (HERG-N) was kindly provided by Jeanne Nerbonne (Washington University, St. Louis, MO) and Amber Pond (Purdue University, W. Lafayette, IN) (Pond & Nerbonne, 2001). An antibody specific to the C terminus of HERG (HERG-C) was obtained from Alomone Labs (APC-062; Jerusalem, Israel). The HERG-N antibody binds to both HERG A and HERG $C_{Cardiac}$ proteins, whereas the HERG-C antibody specifically binds to HERG A only.

### Coimmunoprecipitation of HERG A and HERG $C_{Cardiac}$

Protein extracts were prepared from 20 HERG A/HERG $C_{Cardiac}$ mRNA coinjected oocytes by extraction in 1 ml of radioimmunoprecipitation assay (RIPA) buffer (0.5% [v/v] Nonidet P-40, 150 mm NaCl, 1 mm ethylenediaminetetraacetic acid [EDTA], 50 mm

Tris-HCl [pH 7.5]) with proteinase inhibitors (Roche, Indianapolis, IN) with 200 μl (v/v) of glass beads (0.4 μm). The oocytes were disrupted by 10 cycles of vortexing (30 s vortex/30 s on ice) at 4°C. The detergent extract was clarified by centrifugation at 600 × g for 10 min at 4°C. To 100 μg of detergent-extracted protein in 500 μl of RIPA buffer, 0.5 μg of HERG-C antibody (Alomone Labs) was added. This mixture was rotated overnight at 4°C. Subsequently, 200 μl of protein A sepharose beads (50/50 suspension) in RIPA buffer was added and the mixture rotated overnight at 4°C. Immune complexes were washed three times with RIPA buffer using spin columns (Pierce, Rockford, IL) at 600 × g for 1 min. Finally, immune complexes were eluted from the beads in the spin column using 50 μl of sodium dodecyl sulfate polyacrylamide gel electrophoresis (SDS-PAGE) sample buffer for 5 min, followed by a final spin as above. The eluates were stored at −80°C. The eluates and total detergent extract were separated on SDS-PAGE gels and Western-blotted to nitrocellulose membrane. Equal transfer of proteins to the membrane was confirmed by Ponceau red staining. The membranes were probed with an antibody specific to the N terminus of the HERG A protein (HERG-N, 1 μg/ml working concentration) and secondary detection with anti-rabbit immunoglobulin G horseradish peroxidase and subsequent detection with an enhanced chemiluminescence kit (Amersham, Arlington Heights, IL). In all immunoprecipitation (IP) experiments, cell lysates were precipitated with a HERG A C-terminus-specific antibody and immunoblotted with a HERG N-terminal antibody unless otherwise mentioned.

## Confocal Microscopy of Xenopus Oocytes Injected with HERG $C_{CARDIAC}$

Confocal microscopy was performed on a Bio-Rad (Richmond, CA) MRC 1024 confocal laser scanning microscope using a × 20 objective. GFP fluorescence was selected with the prescribed optical methods of this microscope. All images were recorded at the same settings of laser power and photomultiplier sensitivity (30% laser, no low signal). Images were processed with Adobe Photoshop (Adobe Systems, Mountain View, CA), with identical values for contrast and brightness. Analysis was performed with Leica (Deerfield, IL) confocal software. Fluorescence was quantified using a line profile analysis on 10 oocytes and appeared to be similar in 95% of cells.

## Preparation of Oocytes and Crna Synthesis and Injection

*X. laevis* was anesthetized by immersion in 0.2% 3-aminobenzoic acid ethyl ester (Sigma-Aldrich, Poole, UK). Animals were then killed by cervical dislocation, and oocytes were removed from the ovaries. The follicular membranes were removed following collagenase treatment (collagenase B; Boehringer-Mannheim, Mannheim, Germany) and, in some cases, by an osmotic shock procedure (Pajor, Hirayama & Wright, 1992). cRNA was synthesized from linearized template using the mMESSAGE mMachine kit (Ambion, Austin, TX). cRNA was diluted in Rnase-free water at different ratios to give upon expression an optimal 2–10 μA of outward current. Since the ratio of protein levels of the HERG A and HERG $C_{Cardiac}$ isoform are not known due to the absence of a specific antibody to the HERG $C_{Cardiac}$ isoform, we decided to coexpress the HERG A and HERG $C_{Cardiac}$ isoform at a 1:1 ratio. All recordings were made after 3 days of incubation. Oocytes were cultured at 18°C in storage solution (96 mM NaCl, 2 mM KCl, 1 mM $MgCl_2$, 1.8 mM $CaCl_2$, 5 mM 4-(2-hydroxyethyl)-1-piperazineethanesulfonic acid [HEPES], supplemented with 10 μg/ml gentamicin and 1 mg/ml BSA [pH 7.4]).

## Current Recording and Data Analysis

Currents were recorded using a two-electrode voltage clamp (OC-725C; Warner Equipment, Hamden, CT) and pClamp 9.0 software (Axon Instruments, Foster City, CA). pClamp and Origin 6.1 (Microcal Software, Northampton, MA)were used for data analysis and plotting. The electrode resistance was 0.5–1 MΩ in 2 M KCl. The holding potential was −80 m*V*, and all recordings were done at room temperature, roughly 25°C. Data were routinely discarded if the leak exceeded 10% of the maximum conductance of the expressed currents, but for all the data in this study, the leak currents seen with steps from −80 to −100 m*V* were $<0.2$ μA, $<1\%$ of the maximum current of the expressed channel; therefore, no leak subtraction was utilized.

*I-V* relationships were determined by recording outward current in response to a standard voltage protocol with pulses from −80 to +70 m*V* for 1 s in steps of 10 m*V* from a holding potential of −80 m*V*. Each voltage command was followed by a repolarization to −100 m*V*, eliciting large inward tail currents. *I-V* plots were determined by plotting the current level at the end of the 1-s pulse *vs.* command voltage. The amplitudes of relative current at each corresponding command voltage were normalized to the maximal recorded current.

The *G-V* relationship was determined in response to voltages from −100 to +70 m*V* in 10-m*V* steps from a holding potential of −80 m*V*. Tail currents were fitted to a double-exponential function ($y = A1e - t/1 + A2e - t/2$) and extrapolated to the end of the command voltage. These values were plotted against voltage and fitted with a single-power Boltzmann function of the form $y = 1 - (1/(1 + e(V - V1/2)/k))$. The midpoint is $V1/2$ and $k$ is a slope factor.

Deactivation curves were determined by activating channels from rest (−80 m*V*) with a 1-s pulse to +20 m*V* and measuring the closure of the channels during a range of pulses from 0 to −120 m*V* for 3 s.

Inactivation was measured using a three-pulse voltage protocol. First, channels were fully activated (and inactivated) by a pulse to +60 m*V* for 5 s. During a subsequent pulse to −80 m*V*, channels recovered from inactivation. Then, prior to deactivation, a range of depolarizing potentials from +60 to −20 m*V* was given and channels reentered the inactivated state. The resulting decay traces represent the kinetics of channel inactivation.

Time constants ($\tau$) for the transients were measured by curve fitting with Clampfit (Molecular Devices, Sunnyvale, CA). Data were digitized at 2 or 4 kHz without filtering. Deactivation $\tau$ values were derived from a Chebyshev fit to the deactivating current of the equation $y = A_0 + A_1 e^{-t/\tau 1} + A_2 e^{-t/\tau 2}$. Fitting began within 5 ms of the peak of the tail current, with the first cursor of the fitting window advanced to the first point in time that did not force a fit to the recovery phase; the second cursor was at the end of the 1.5-s pulse. The deactivation traces were best fit with two exponentials. The inactivation time constant was similarly derived from a fit of the equation $y = A_e - t/\tau$ to the inactivating current. In this case, the fitting window began as soon as the clamp settled, approximately 2 ms, and continued to the end of the 300-ms pulse.

A model AP pulse paradigm was used. APs were evoked by passing brief current pulses (1 ms, 1.2 times threshold) at a frequency of 1 Hz through the recording electrode with an active bridge circuit at −80 m*V*. Mean amplitudes of each evoked AP current were calculated from the peak current between dotted lines. Repolarization $\tau$ values were derived from the double exponential fitted ($f[t] = \sum_{i=1} n = 2\, Aie^{-t/\tau i} + mt + C$) repolarization currents between two dotted lines.

### Statistical Analysis

All data were calculated as mean ± standard error of the mean (SEM; $N$ = number of oocytes tested, $n$ = number of times experiments were repeated). Statistical comparisons of multiple means in plots of variables *vs*. voltage were performed using one-way ANOVA. Differences were considered statistically significant at $P \leq 0.05$; $F$ values were also included in order to provide additional information on the degree of statistical significance. (The $P$ value is the probability of obtaining a greater value for $F$ by chance alone. Because the $P$ value is smaller than the significance level $\alpha$, we conclude that at least one of the means is significantly different from the others).z

## Results

### HERG $C_{CARDIAC}$ Splicing Site

HERG $C_{Cardiac}$, which was originally isolated from a human infant brain EST library, lacked the last 359 amino acids of HERG A and had a unique 89-amino acid C-terminal end (Fig. 1a); it appears to result from an alternate polyadenylation site between exons 9 and 10 (London et al., 1998). A BLAST homology search indicated 100% homology to $HERG_{USO}$ (Kupershmidt et al., 1998).

### Expression of HERG $C_{CARDIAC}$ in Human Heart and Ventricles

Real-time PCR experiments in total human heart and ventricular tissue revealed that the HERG $C_{Cardiac}$/HERG A mRNA mean comparative expression ratio was 6.4 in total heart tissue and 4 in human ventricular tissue. The HERG $C_{cardiac}$ PCR product was cloned into pGEM-T (Promega), and the plasmids from 10 positive colonies were sequenced to confirm the identity of the PCR products (*data not shown*). This indicated that the HERG $C_{Cardiac}$ isoform was more abundant than the HERG A isoform (Fig. 1b, $n = 5$; means of comparative expression values were statistically significant; $F = 21.7$, $P = 0.04$).

### Expression and Localization of HERG $C_{CARDIAC}$ in *X. laevis* Oocytes

In order to determine the expression and localization of HERG $C_{Cardiac}$ in *X. laevis* oocytes, we constructed a HERG $C_{Cardiac}$-GFP chimera. Imaging studies with confocal microscopy demonstrated that the HERG $C_{Cardiac}$-GFP construct showed an identical expression pattern to Kv1.4–GFP, which was predominantly in the oocyte plasma membrane. In contrast, the HERG $C_{Cardiac}$-GFP expression pattern was not similar to that of GFP alone (Fig. 2a; $n = 6$, $N = 40$). Fluorescence intensity plots of line profile analyses of representative images are shown in Figure 2.

### Functional Expression Studies

We performed a number of molecular and electrophysiogical studies in order to confirm the functional expression of HERG $C_{Cardiac}$ in *X. laevis* oocytes.

#### *Kinetics of HERG $C_{Cardiac}$ and HERG $C_{Cardiac}$ + HERG A Heteromultimeric Channels*

*I-V and steady-state activation (G-V) relationships*. Representative traces recorded from oocytes injected with Rnase-free water or heterologously expressing HERG A, HERG $C_{Cardiac}$ *and HERG* $C_{Cardiac}$ + HERG A heteromultimeric channels are shown in Figure 3a. HERG $C_{Cardiac}$ channel-expressing oocytes demonstrated smaller noninactivating outward currents and shorter tail currents compared to those of HERG A channels in response to a depolarizing pulse paradigm (Fig. 3a; $N = 50$, $n = 5$). Oocytes expressing equal amounts of HERG $C_{Cardiac}$ + HERG A heteromultimeric channels had intermediate levels of outward currents and tail currents compared to those of HERG A and HERG $C_{Cardiac}$ alone, indicating the possible coassembly of HERG A channel subunits with HERG $C_{Cardiac}$ channel subunits (Fig. 3a; $N = 65$, $n = 7$).

*I-V* (current-voltage) plots for homomeric HERG $C_{Cardiac}$ channel currents showed significant reductions in mean amplitudes compared to homomeric HERG A channel currents (Fig. 3b; $N = 20$, $n = 5$, $F = 3.6$, $P = 0.05$). Inward rectification seemed to be diminished (Fig. 3c). Moreover, HERG $C_{Cardiac}$ + HERG A heteromultimeric channels showed significant reductions in mean amplitudes compared to homomeric HERG A channel currents (Fig. 3b; $N = 20$, $n = 5$, $F = 4.3$, $P = 0.047$). In addition, inward rectification of HERG $C_{Cardiac}$ + HERG A heteromultimeric channels was reduced (Fig. 3c).

*G-V* (conductance-voltage) plots for homomeric HERG $C_{Cardiac}$ channel currents were shifted toward a depolarizing direction, and slope values were also altered ($V1/2 = -2.5 \pm 4.4$ m$V$ slope = $31.8 \pm 5.9$; $N = 20$, $n = 5$; Fig. 4). For heteromultimeric HERG $C_{Cardiac}$ + HERG A channels, *G-V* plots were also significantly shifted toward a more hyperpolarized direction but with a different slope value compared to homomeric HERG A channels ($V1/2 = -31.5 \pm 1$ m$V$, slope = $7.8 \pm 0.6$, $F = 3.6$, $P = 0.002$ for homomeric HERG A channels and $V1/2 = -33.6 \pm 2$ m$V$, slope = $12.2 \pm 1$, $F = 3.3$, $P = 0.047$ for homomeric HERG $C_{Cardiac}$ channes; $N = 20$, $n = 5$; Fig. 4). These data indicated the formation of heteromeric channels between HERG A and HERG $C_{Cardiac}$ channels with activation kinetics resembling neither those of HERG A homomers nor those of HERG $C_{Cardiac}$ homomers.

*Deactivation kinetics of HERG $C_{Cardiac}$ and HERG $C_{Cardiac}$ + HERG A heteromultimeric channels*. Representative deactivation traces recorded from oocytes heterologously expressing HERG A, HERG $C_{Cardiac}$

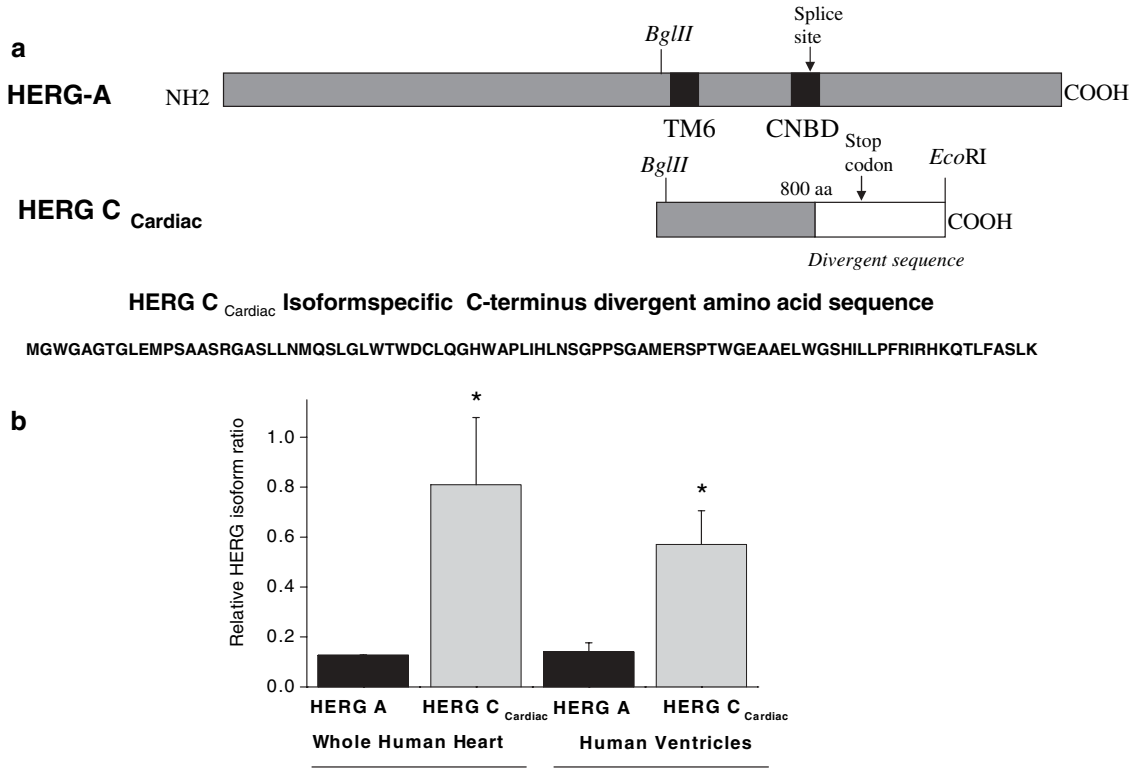


**Fig. 1.** HERG $C_{cardiac}$ splicing site, divergent amino acid sequence and expression levels in human heart. (*a*) Schematic representation of HERG $C_{Cardiac}$ isoform showing the splicing site, plasmid construction and divergent amino acid sequence. (*b*) Real-time PCR data, illustrating relative HERG isoform ratio of HERG $C_{Cardiac}$ and HERG A mRNAs in total human heart and ventricular tissue. *Means of comparative expression levels of HERG $C_{Cardiac}$ and HERG A mRNAs were significantly different at $P \leq 0.05$.

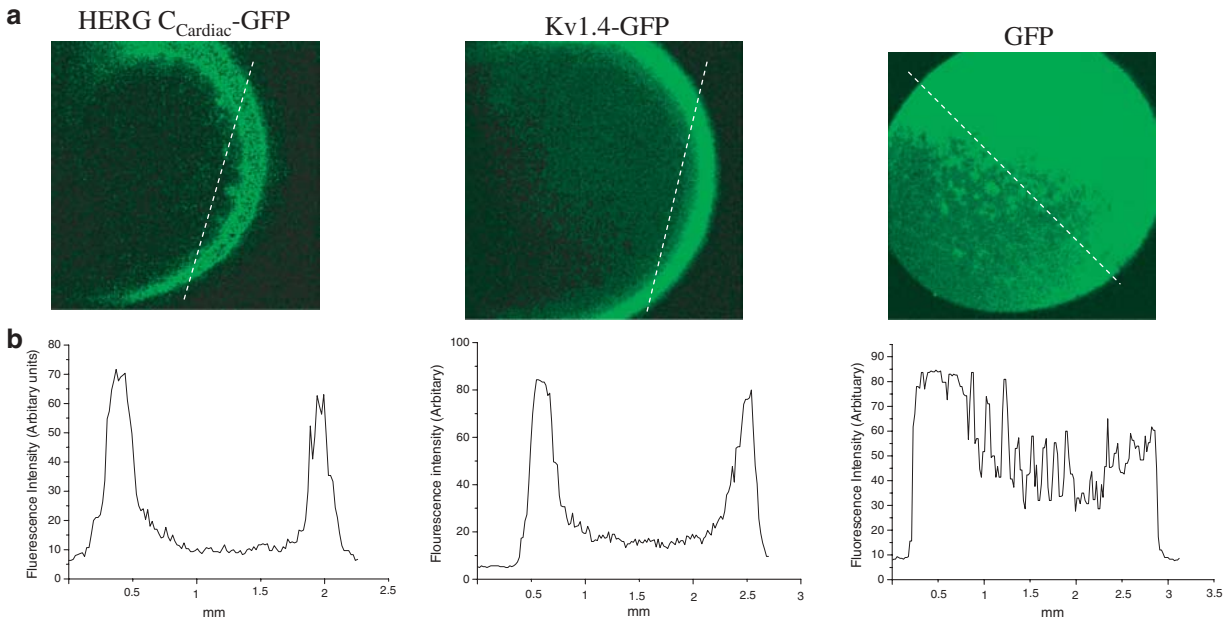


**Fig. 2.** Expression and localization of HERG $C_{Cardiac}$ in *X. laevis* oocytes. (*a*) HERG $C_{Cardiac}$-GFP construct showed an identical expression pattern to Kv1.4 –GFP, which was mainly in the oocyte plasma membrane; in contrast, the HERG $C_{Cardiac}$-GFP expression pattern was not similar to that of cytoplasmic GFP protein. (*b*) Fluorescence intensity plots of line profile analysis of corresponding images in *a*.

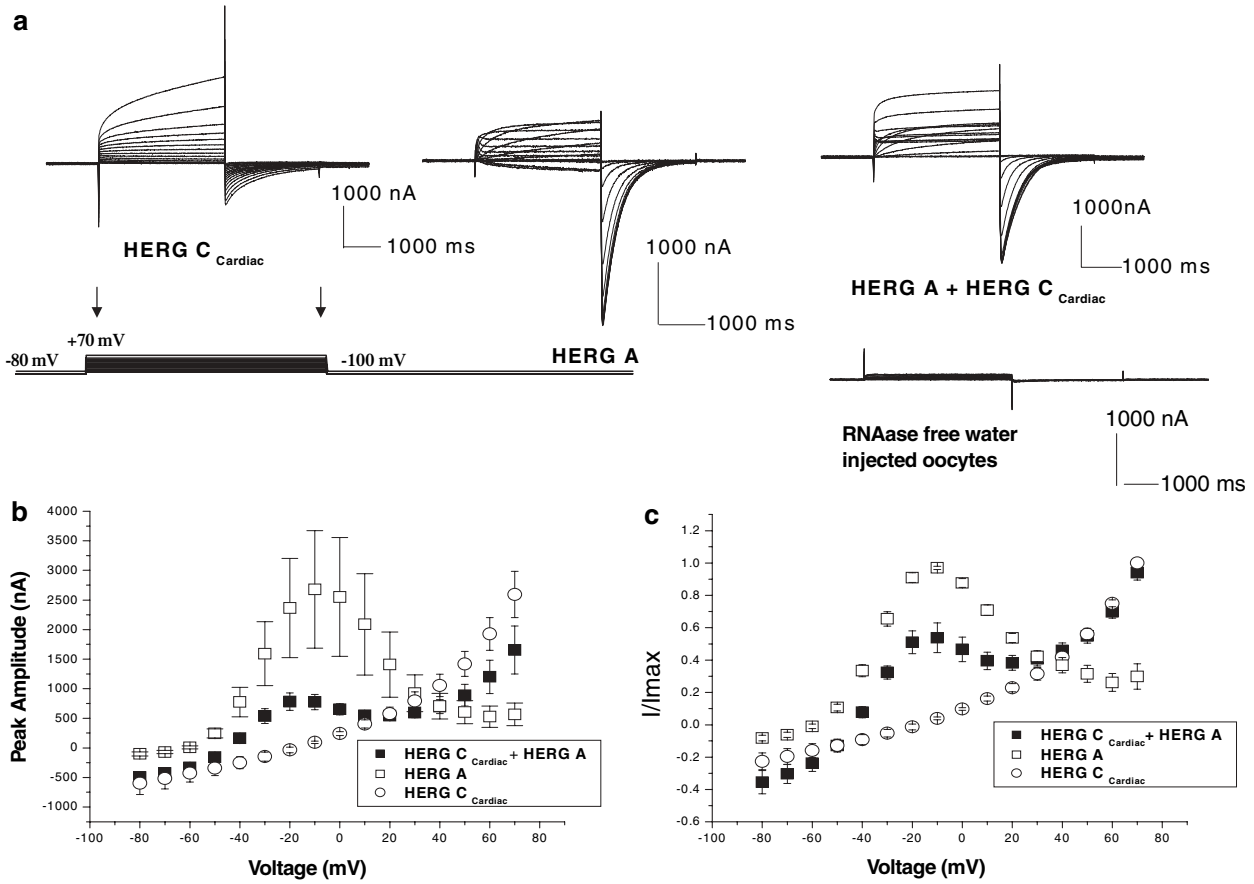


**Fig. 3.** Functional expression of HERG $C_{Cardiac}$, HERG A and HERG $C_{Cardiac}$ + HERG A channels in *X. laevis* oocyte membranes. (*a*) Representative current traces recorded from RNase-free water-injected oocytes of HERG A homomeric, HERG $C_{Cardiac}$ homomeric and HERG A + HERG $C_{Cardiac}$ heteromeric channels expressed in oocytes. Pulse protocol indicated below. (*b*) Peak amplitude *I-V* plots for HERG A and HERG $C_{Cardiac}$ homomeric and HERG A + HERG $C_{Cardiac}$ heteromeric channels expressed in oocytes. HERG $C_{Cardiac}$ channel currents showed significant reductions in mean amplitude compared to homomeric HERG A channel currents. (*c*) Normalized current-voltage plots for HERG A and HERG $C_{Cardiac}$ homomeric and HERG A + HERG $C_{Cardiac}$ heteromeric channels expressed in oocytes.

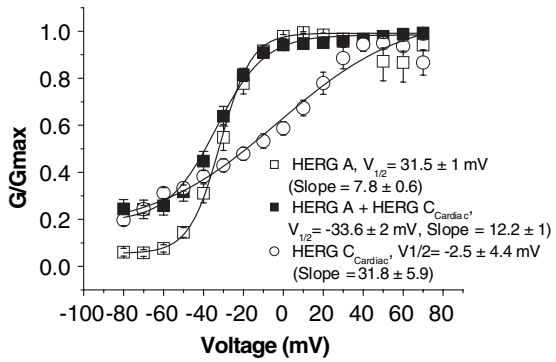


**Fig. 4.** Steady-state activation kinetics of HERG $C_{Cardiac}$, HERG A and HERG $C_{Cardiac}$ + HERG A channels. *G-V* plots for HERG A and HERG $C_{Cardiac}$ homomeric and HERG A + HERG $C_{Cardiac}$ heteromeric channels expressed in oocytes. Steady-state activiation curves for HERG $C_{Cardiac}$ and HERG A homomeric and HERG A + HERG $C_{Cardiac}$ heteromeric channels. *G-V* plots of HERG A + HERG $C_{Cardiac}$ heteromeric channels are shifted toward a depolarizing direction with different slope values.

and HERG $C_{Cardiac}$ + HERG A heteromultimeric channels are shown in Figure 5a. Overall, homomeric HERG $C_{Cardiac}$ channels expressed in oocytes demonstrated statistically faster deactivation than those of homomeric HERG A channels at −120 m*V* (Fig. 5a). Fast (Fig. 5b, $N = 20$ for each homomeric construct at all tested voltages, −80 to −120 m*V*, $F = 9.9$, $P = 0.01$) and slow deactivation values of homomeric HERG $C_{Cardiac}$ channels were significantly faster than those of homomeric HERG A channels at all tested voltages (Fig. 5c, $N = 20$ for each homomeric construct, $F = 5.7$, $P = 0.04$, $n = 6$). Additionally, HERG A homomeric and HERG $C_{Cardiac}$ + HERG A heteromultimeric channels expressed in oocytes had significant changes in deactivation compared to homomeric HERG $C_{Cardiac}$ channels only ($N = 20$ for each construct, $n = 6$, $F = 5.0$, $P = 0.02$ for fast deactivation; $F = 7.5$, $P = 0.02$, HERG A homomers *vs.* HERG $C_{cardiac\ homomers}$; $F = 5.7$, $P = 0.044$, HERG Ccardiac homomers *vs.* HERG $C_{Cardiac}$ + HERG A heteromers for slow deactivation; Fig. 5b, c). However, the slow deactivation $\tau$ values of these heteromers were not significantly different from HERG A. For example, fast deactivation $\tau$ values at −120 m*V* were 30.0 ± 8.5 for HERG A, 17.6 ± 7.8 for HERG

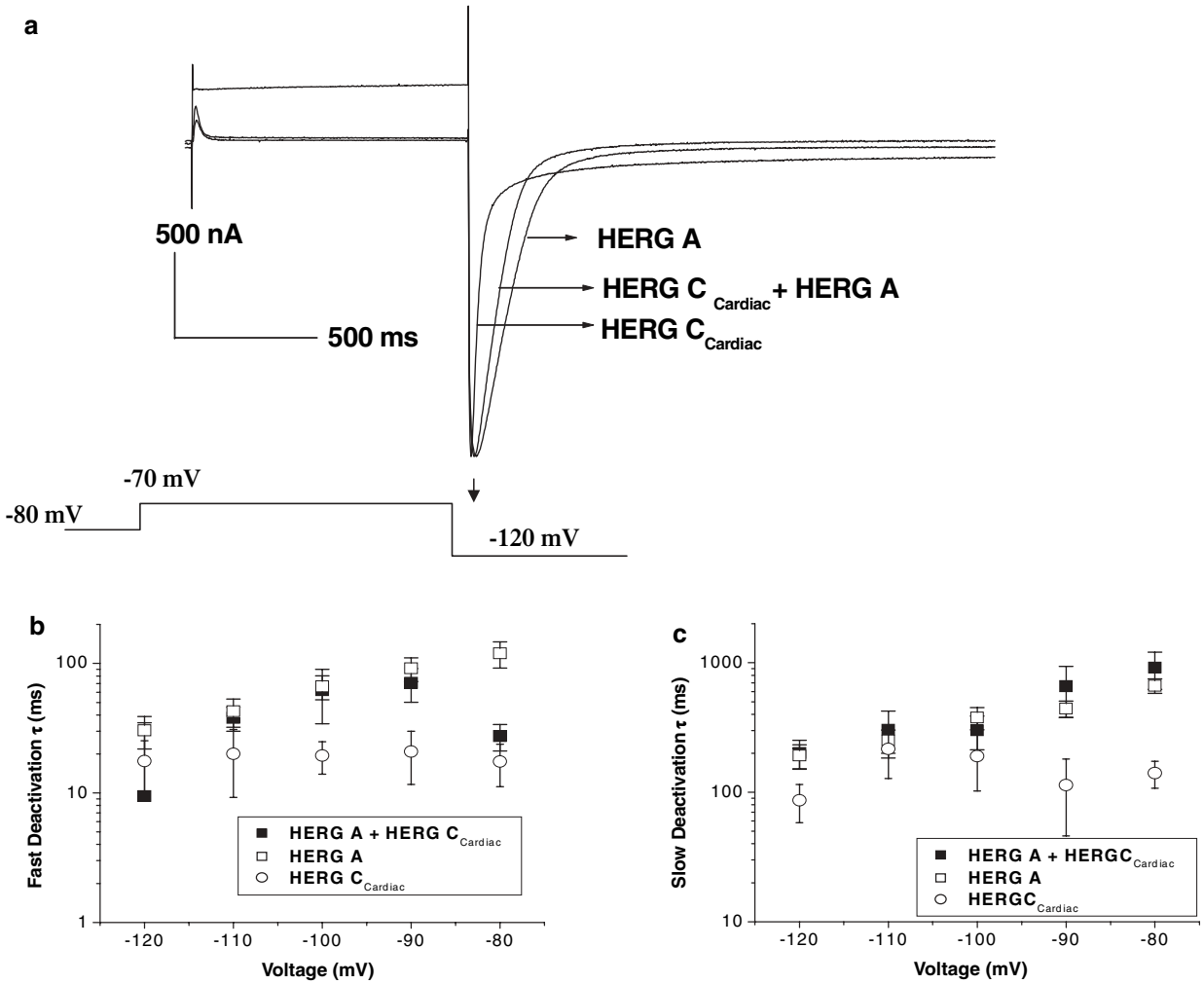


**Fig. 5.** Deactivation kinetics of HERG $C_{Cardiac}$, HERG A and HERG $C_{Cardiac}$ + HERG A channels. (*a*) Representative normalized deactivation traces recorded from oocytes heterologously expressing HERG A, HERG $C_{Cardiac}$, and HERG $C_{Cardiac}$ + HERG A heteromultimeric channels are illustrated. Pulse protocol is indicated below traces. Homomeric HERG $C_{Cardiac}$ channels expressed in oocytes demonstrated statistically faster deactivation than those of homomeric and heteromeric channels. (*b*) Plot of fast deactivation $\tau$ values vs. voltage for HERG A ans HERG $C_{Cardiac}$ homomeric channels and HERG $C_{Cardiac}$ + HERG A heteromultimeric channels. (*c*) Plot of slow deactivation $\tau$ vs. voltage for HERG A and HERG $C_{Cardiac}$ homomeric channels and HERG $C_{Cardiac}$ + HERG A heteromultimeric channels. Slow $\tau$ values were statistically (one-way ANOVA) shorter in HERG $C_{Cardiac}$ homomeric channels when compared with HERG $C_{Cardiac}$ + HERG A heteromultimeric and HERG A homomeric channels. However, slow $\tau$ values of these heteromultimers were not statistically significant from those of the HERG A homomeric channel.

$C_{Cardiac}$ and 9.4 ± 25.4 for HERG $C_{Cardiac}$ + HERG A heteromultimeric channels, whereas slow deactivation $\tau$ values were 191.9 ± 40.1, 86.5 ± 28.3 and 200.9 ± 50.9, respectively.

*Inactivation kinetics of HERG $C_{Cardiac}$ and HERG $C_{Cardiac}$ + HERG A heteromultimeric channels.* Representative inactivation traces recorded from oocytes heterologously expressing HERG A, HERG $C_{Cardiac}$ and HERG $C_{Cardiac}$ + HERG A heteromultimeric channels are shown in Figure 6a. Overall, homomeric HERG $C_{Cardiac}$ and heteromeric HERG $C_{Cardiac}$ + HERG A channels expressed in oocytes demonstrated statistically slower inactivation $\tau$ values than those of homomeric HERG A channels at all tested voltages ($F = 2.9$, $P = 0.05$; Fig. 6b). Inactivation $\tau$ values of HERG $C_{Cardiac}$ + HERG A heteromultimeric channels expressed in oocytes were approximately twofold slower than those of homomeric HERG A channels and HERG $C_{Cardiac}$ at all tested voltages (e.g., at +60 m*V* HERG A homomer inactivation $\tau$ was 3.0 ± 0.4 ms and heteromer inactivation $\tau$ was 6.0 ± 0.8 ms; $N = 15$ for each construct, $n = 5$; Fig. 6b, c). These channel kinetics data led us to pursue IP experiments in order to reconfirm formation of heteromultimers between HERG A and HERG $C_{Cardiac}$ channel isoforms.

## *Molecular Association between HERG A and HERG $C_{Cardiac}$ Channel Proteins*

IP experiments with a HERG C-terminal antibody demonstrated that HERG A and HERG $C_{Cardiac}$ channel proteins were associated (Fig. 7, $n = 5$). In

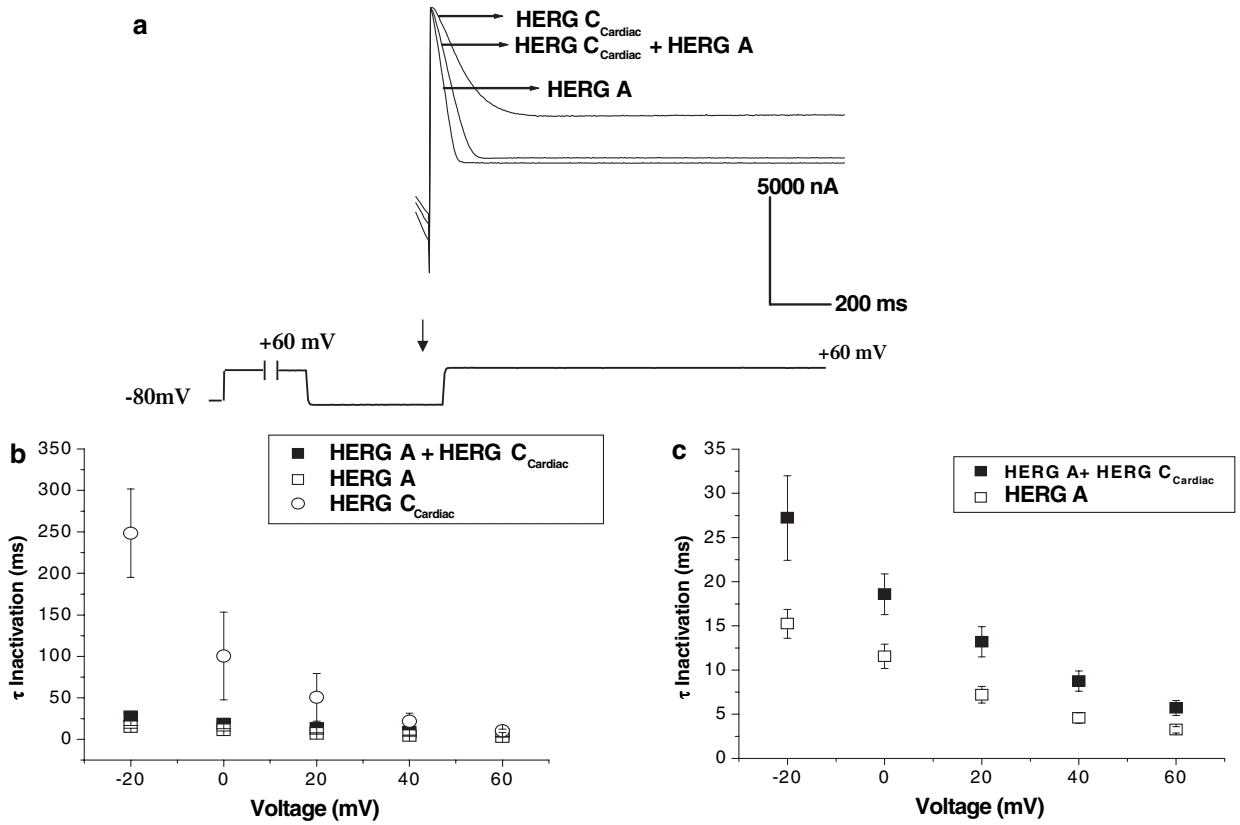


**Fig. 6.** Inactivation kinetics of HERG $C_{Cardiac}$ homomeric and HERG $C_{Cardiac}$ + HERG A heteromultimeric channels. (*a*) Inactivation pulse protocol and corresponding current traces recorded from oocytes heterologously expressing HERG A and HERG $C_{Cardiac}$ homomeric and HERG $C_{Cardiac}$ + HERG A heteromultimeric channels are shown. Pulse protocol is indicated below traces. (*b*) Inactivation plots for HERG A or HERG $C_{Cardiac}$ homomeric channels and HERG A + HERG $C_{Cardiac}$ heteromultimeric channels. (*c*) Inactivation plot for HERG $C_{Cardiac}$ homomeric and HERG A + HERG A $C_{Cardiac}$ heteromultimeric channels.

oocytes coexpressing both HERG A and HERG $C_{Cardiac}$, two protein bands were observed in whole-cell lysates of approximately 140 and 100 kDa. The predicted sizes of HERG A and HERG $C_{Cardiac}$ are 127 and 98 kDa, respectively. The same bands were also observed in the IP reaction, suggesting molecular association between these two isoforms. Two bands, of 140 and 100 kDa, were observed in IP reactions only when HERG A and HERG $C_{Cardiac}$ were coinjected and an antibody specific to the HERG A channel was used in the IP reaction. Furthermore, Western blot data confirmed the existence of HERG $C_{Cardiac}$ protein in *X. laevis* oocyte membranes expressing only HERG $C_{Cardiac}$ cRNA (Fig. 7, lane 3).

### *Modulation of Model AP by HERG A + HERG $C_{Cardiac}$ Channel Heteromers*

There is now substantial evidence that HERG A and its isoforms modulate the cardiac AP in heart (London et al., 1997; Mitcheson & Sanguinetti, 1999; Jones et al., 2004). In this study, we aimed to identify the contribution of HERG $C_{Cardiac}$ to cardiac AP; therefore, we applied an AP paradigm to HERG A + HERG $C_{Cardiac}$ heteromeric channels and HERG A homomeric channels.

Application of a model AP pulse paradigm to heterologously expressed HERG A homomeric and HERG A + HERG $C_{Cardiac}$ heteromeric channels in oocytes resulted in a typical AP current whose kinetics differed from those of HERG A homomeric currents when compared to HERG A + HERG $C_{Cardiac}$ heteromeric channels (Fig. 8a, b; $N = 50$ for each construct, $n = 7$). An AP analysis diagram is shown in Figure 8c.

*Effects of HERG A + HERG $C_{Cardiac}$ channel heteromers on mean repolarization amplitude.* In HERG A + HERG $C_{Cardiac}$ channel heteromers expressed in oocytes, mean amplitudes of recorded model AP were significantly two and half times decreased compared to HERG A homomeric channels (mean amplitudes of AP determined by calculating the maximum current recorded between two dotted lines indicated in Fig. 8c, d). The mean amplitudes of the model AP were 938.3 ± 180.5 for heteromeric and 2,345.0 ± 599.4 for homomeric channels ($N = 50$, $n = 7$, $F = 5.0$,

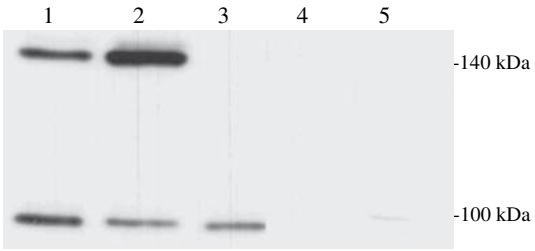


**Fig. 7.** Molecular interactions between HERG $C_{Cardiac}$ and HERG A channels in *X. laevis* oocyte membranes. Western blot with HERG N-terminal antibody illustrating the molecular association between HERG A and HERG $C_{Cardiac}$ channel proteins. In all IP experiments, cell lysates were precipitated with HERG C-terminal antibody and immunoblotted with HERG N-terminal antibody unless otherwise mentioned. Lane 1, whole-cell lysate from oocytes coinjected with HERG A and HERG $C_{Cardiac}$ mRNAs (1:1 ratio); lane 2, IP performed from whole-cell lysates of oocytes expressing functional HERG $C_{Cardiac}$ /HERG A heteromultimeric channels (confirmed with electrophysiological experiments); lane 3, whole-cell lysate from oocytes expressing only functional HERG $C_{Cardiac}$ channels; lane 4, IP performed in oocytes expressing only functional HERG $C_{Cardiac}$ channels; lane 5, IP performed on oocytes coinjected with HERG A and HERG $C_{Cardiac}$ mRNAs (1:1 ratio) with no IP antibody used. Predicted size in kilodaltons is indicated.

$P = 0.050$), indicating a possible contribution of the HERG $C_{Cardiac}$ channel splice variant to the mean amplitude of model AP.

*Effects of HERG A + HERG $C_{Cardiac}$ channel heteromers on repolarization $\tau$.* For HERG A + HERG $C_{Cardiac}$ channel heteromers, the recorded fast and slow repolarization $\tau$ values of model AP were significantly increased compared to those of HERG A homomeric channels (Fig. 8e, f; $N = 14$, $n = 4$, $F = 8.6$, $P = 0.02$ for fast repolarization $\tau$; $F = 7.3$, $P = 0.03$ for slow repolarization $\tau$). The fast repolarization $\tau$ values were $3.8 \pm 0.06$ for HERG A homomeric channels and $4.23 \pm 0.1$ for heteromers, whereas the slow repolarization $\tau$ values were $10.13 \pm 0.43$ for HERG A homomers and $13.24 \pm 1.0$ for heteromers. The increase was 13.15% for fast repolarization and 30.70 % for slow repolarization.

## Discussion

In the present work, we explored the expression and channel kinetics of HERG $C_{Cardiac}$ channel isoforms in the *X. laevis* oocyte expression system.

Our findings indicated that in human total heart tissue mRNA levels of the HERG $C_{Cardiac}$ isoform were 6.4 times more than those of the HERG A isoform. These data were consistent with previous Northern blot studies from human muscle and brain (London et al., 1998) and human heart (Kupershmidt et al., 1998) tissues. At present, we are developing an antibody to the HERG $C_{Cardiac}$ isoform in order to determine if this RNA transcription level results in a similar level of protein expression in the human heart. However, heterologous expression of this isoform in *Xenopus* oocytes indicated that it was able to form functional channel protein. This was confirmed by Western blotting of whole-cell lysates prepared from *X. laevis* oocytes injected with the HERG $C_{Cardiac}$ isoform and by electrophysiology. Our findings together with the previous studies on this isoform suggest that the HERG $C_{Cardiac}$ isoform may be expressed throughout all human tissues (London et al.,1998); it is especially abundant in human heart and jejunum (London et al., 1998; Farelly et al., 2003) and is likely to contribute to the physiological function of HERG channels in these tissues. However, our study does not directly show that the HERG $C_{Cardiac}$ isoform is trafficked to the plasma membrane in human heart. However, we aim to resolve this issue in the future by use of a HERG $C_{Cardiac}$-specific antibody, which we are currently developing.

Conflicting results have been reported for the expression of $HERG_{USO}$ channels in mammalian cells. Kupershmidt et al. (1998) did not observe functional homomeric channels in $Ltk^-$ cells, whereas Farrelly et al. (2003) demonstrated functional expression of $HERG_{USO}$ channels together with HERG A in human jejunum. Our functional expression data strongly resemble the data obtained by Farrelly et al. (2003) since both systems detected functional current. The other fact is that most of the HERG-related channels were initially expressed in *Xenopus* oocytes. All these studies demonstrate that the *Xenopus* oocyte is a reliable and reputable system for HERG-expression studies (Warmke & Ganetzky, 1994; Sanguinetti et al., 1995; Trudeau et al., 1995). Our study demonstrated that $HERG_{USO}$ (HERG $C_{Cardiac}$) is able to form functional homomeric channels in *Xenopus* oocytes; therefore, further studies may prefer this expression system.

Our results demonstrated that HERG $C_{Cardiac}$ was able to form functional homomeric channels in the membrane of oocytes with different activation, deactivation and inactivation kinetics, which were similar to the deactivation and activation kinetics of HERG A C-deleted constructs (HERGCΔ278, HERGCΔ236; Aydar & Palmer, 2001). However, the inactivation kinetics in this study of C-deleted constructs expressed in oocytes was not altered (Aydar & Palmer, 2001).

HERG $C_{Cardiac}$ homomeric channels had slower inactivation than HERG A homomers. This could be due to the addition of a novel unique HERG $C_{Cardiac}$ splicing sequence (containing 13 charged amino acids). The mean amplitude of functional homomeric HERG $C_{Cardiac}$ channel currents was

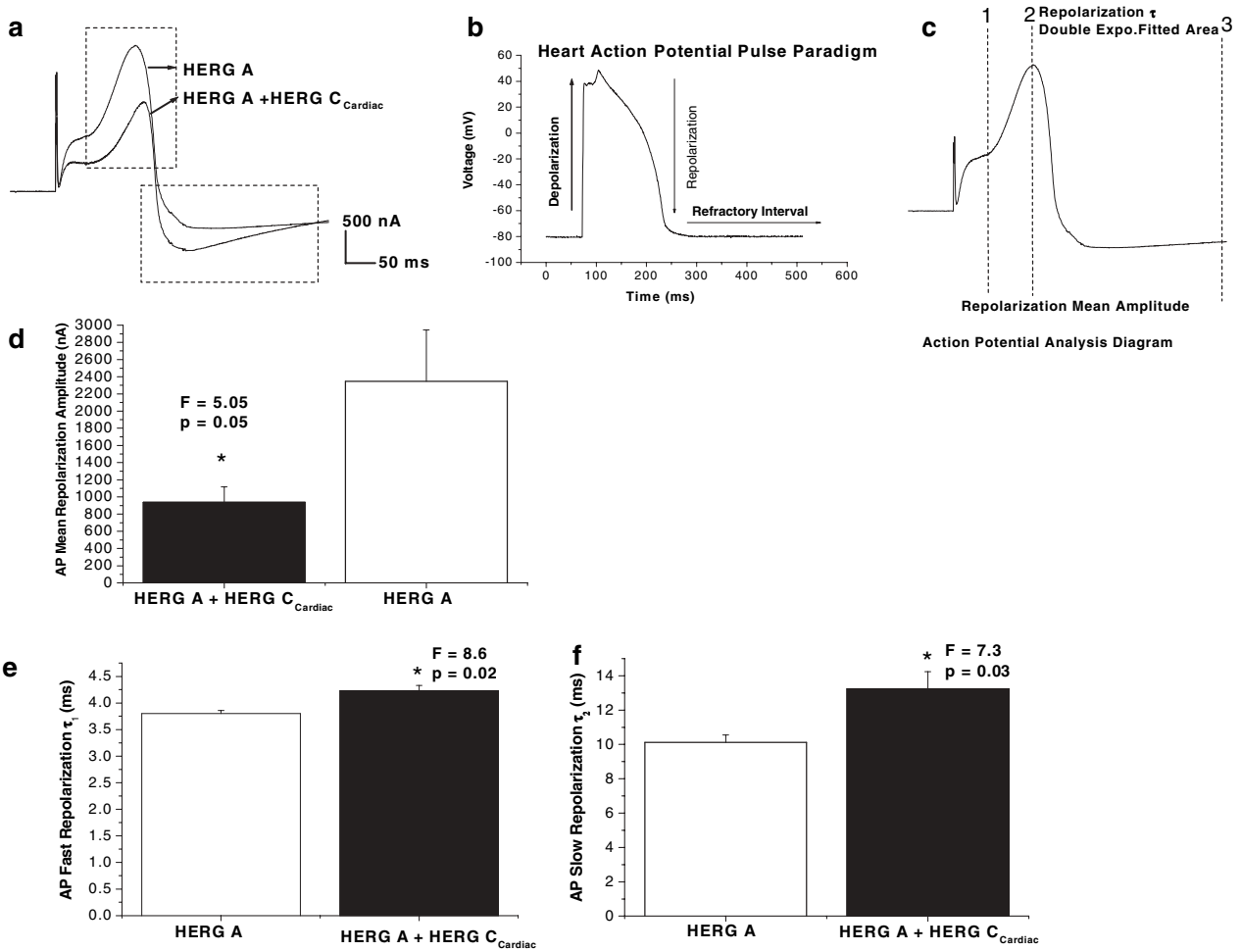


**Fig. 8.** Modulation of model cardiac AP by HERG A + HERG $C_{Cardiac}$ channel heteromers. (*a*) Representative AP current traces recorded from HERG A homomeric and HERG A + HERG $C_{Cardiac}$ heteromeric channels. *Dotted rectangular area at top of traces* illustrates repolarization mean amplitudes and *dotted rectangular area at bottom of traces* illustrates repolarization $\tau$ (*b*) Model AP pulse paradigm. (*c*) AP analysis diagram; parts of trace from which repolarization mean amplitudes were calculated are the *dotted lines between 1 and 3*, whereas parts of trace from which repolarization $\tau$ values were calculated are *dotted lines between 2 and 3*. (*d*) AP mean repolarization amplitude bar graphs recorded from HERG A homomeric and HERG A + HERG $C_{Cardiac}$ heteromeric channels expressed in oocytes. In HERG A + HERG $C_{Cardiac}$ channel heteromers, mean amplitudes of recorded model AP are approximately two and half times decreased compared to HERG A homomeric channels. (e) Bar graph of mean fast repolarization $\tau$ values for HERG A homomeric and HERG A + HERG $C_{Cardiac}$ heteromeric channels expressed in oocytes. (f) Bar graph of mean slow repolarization $\tau$ for HERG A homomeric and HERG A + HERG $C_{Cardiac}$ heteromeric channels expressed in oocytes.

drastically reduced compared to HERG A homomers. Inward rectification also seemed to be diminished.

The present study proved that HERG $C_{Cardiac}$ was able to coassemble with the HERG A isoform in order to form HERG A + HERG $C_{Cardiac}$ heteromultimers in *X. laevis* oocytes. This was reconfirmed both with functional expression and with IP studies. HERG A + HERG $C_{Cardiac}$ heteromultimers had statistically different steady-state activation (Kupershmidt et al., 1998), deactivation and inactivation kinetics than those of HERG A and HERG $C_{Cardiac}$ homomeric channels.

These data are consistent with those of Kupershmidt et al. (1998) on $HERG_{USO}$ expressed in $Ltk^-$ cells and on HERG A C-terminal deletions expressed in oocytes (Aydar & Palmer, 2001). Our data indicated that these heteromers possessed different channel kinetics, resembling neither those of HERG $C_{Cardiac}$ homomeric channels nor those of HERG A channels. IP experiments with a HERG N-terminal antibody reconfirmed molecular association between these two isoforms. This was previously suggested by Sanguinetti & Jurkiewicz (1990), Kupershmidt et al. (1998), Pond & Nerbonne (2001) and Farrelly et al. (2003).

Our findings on the shift of steady-state activation curves to more negative potentials in the heteromultimeric channels and the decrease of mean amplitude in HERG A + HERG $C_{Cardiac}$ heteromultimers suggest that there could be a considerable amount of similarity between HERG $C_{Cardiac}$ and MinK, which was also demonstrated to be associated with KVLQT1 and HERG proteins and found to modulate cardiac AP (Barhanin et al., 1996; McDonald et al., 1997). MinK, just like HERG $C_{Cardiac}$, can modulate the expression levels of HERG A channels by shifting the steady-state activation to more negative and the steady-state inactivation to more positive voltages when they are coexpressed in *Xenopus* oocytes (McDonald et al., 1997).

HERG channels are best known for their contribution to cardiac AP via recovering from inactivation and remain open long enough to significantly contribute to further repolarization (Sanguinetti et al., 1995; Mitcheson & Sanguinetti, 1999). $I_{Kr}$ is characterized by rapid activation at –30 m$V$ and strong inward rectification at positive potentials, which is due to rapid voltage-dependent C-type inactivation (Sanguinetti & Jurkiewicz, 1990; Yellen, 2002; Tseng, 2001). Inward rectification is due to the faster development of channel inactivation than channel activation at positive potentials, which limits the amount of time that channels spend in the open state (Tseng, 2001). $I_{Kr}$ plays an important role in governing the refractory period of the cardiac AP via increasing the rate of recovery from inactivation through the open state on the repolarization and, at negative voltages, resulting in a large outward current that promotes phase 3 of repolarization.

HERG has electrophysiological properties similar, but not identical, to $I_{Kr}$ (Sanguinetti et al., 1995). The time constants of activation and deactivation of HERG are four to 10 times slower than those of native $I_{Kr}$ as expressed in guinea pig and mouse cardiac myocytes (Sanguinetti & Jurkiewicz, 1990). However, human cardiac myocytes have different cardiac physiology than pig and mouse cardiac myocytes (Nerbonne, 2000). Thus, it is difficult to interpret or compare our data with these studies.

The present study demonstrates that coexpression of the HERG $C_{Cardiac}$ isoform to HERG A channels resulted in a mean reduction of the repolarization current amplitude and increase in the repolarization $\tau$, which suggests a contribution and ability of the HERG $C_{Cardiac}$ isoform to modulate cardiac AP. Therefore, considering the expression levels in heart, coimmunoprecipitation, localization and kinetics of HERG A + HERG $C_{Cardiac}$ heteromultimeric channels, we can speculate that these heteromers are likely to contribute considerably to the physiology of cardiac and other HERG channels.

Alterations of HERG $C_{Cardiac}$ levels may affect the properties of $I_{Kr}$ and modulate the Q-T interval in response to physiological and pathological conditions. In addition, it could provide insight into the exact function of HERG channels in human heart and elsewhere. The expression and functional characterization of this cardiac isoform are likely to be valuable for diagnosis and therapy of inherited cardiac arrhythmia of long Q-T syndrome 2 (Curran et al., 1995; Nerbonne, 2000).

We thank Drs. J. M. Nerbonne and A. Pond for kindly providing the HERG N-terminal antibody.

## References

Aydar, E., Palmer, C. 2001. Functional characterization of the C-terminus of the human ether-a-go-go-related gene $K^+$ channel (HERG). *J. Physiol.* **534:**1–14

Barhanin, J., Lesage, F., Guillemare, E., Fink, M., Lazdunski, M., Romey, G. 1996. K(V)LQT1 and lsK (minK) proteins associate to form the $I_{Ks}$ cardiac potassium current. *Nature* **384:**78–80

Curran, M.E., Splawski, I., Timothy, K.W., Vincent, G.M., Green, E.D., Keating, M.T. 1995. A molecular basis for cardiac arrhythmia: HERG mutations cause long QT syndrome. *Cell* **80:**795–803

Farrelly, A.M., Ro, S., Callaghan, B.P., Khoyi, M.A., Fleming, N., Horowitz, B., Sanders, K.M., Keef, K.D. 2003. Expression and function of KCNH2 (HERG) in the human jejunum. *Am. J. Physiol.* **284:**G883–G895

Jones, E.M., Roti, E.C., Wang, J., Delfosse, S.A., Robertson, G.A. 2004. Cardiac $I_{Kr}$ channels minimally comprise hERG 1a and 1b subunits. *J. Biol. Chem.* **279:**44690–44694

Kupershmidt, S., Snyders, D.J., Raes, A., Roden, D.M. 1998. A $K^+$ channel splice variant common in human heart lacks a C-terminal domain required for expression of rapidly activating delayed rectifier current. *J. Biol. Chem* **273:**27231–27235

Kupershmidt, S., Yang, T., Chanthaphaychith, S., Wang, Z., Towbin, J.A., Roden, D.M. 2002. Defective human ether-a-go-go-related gene trafficking linked to an endoplasmic reticulum retention signal in the C terminus. *J. Biol. Chem.* **277:**27442–27448

London, B., Aydar, E., Lewarchik, C.M., Seibel, J.S., January, C.T., Robertson, G.A. 1998. N- and C-terminal isoforms of HERG in the human heart. *Biophys. J.* **74:**A26

London, B., Trudeau, M.C., Newton, K.P., Beyer, A.K., Copeland, N.G., Gilbert, D.J., Jenkins, N.A., Satler, C.A., Robertson, G. A. 1997. Two isoforms of the mouse ether-a-go-go-related gene coassemble to form channels with properties similar to the rapidly activating component of the cardiac delayed rectifier $K^+$ current. *Circ. Res.* **81:**870–878

McDonald, T.V., Yu, Z., Ming, Z., Palma, E., Meyers, M.B., Wang, K.W., Goldstein, S.A., Fishman, G.I. 1997. A minK-HERG complex regulates the cardiac potassium current $I_{Kr}$. *Nature* **388:**289–292

Mitcheson, J.S., Sanguinetti, M.C. 1999. Biophysical properties and molecular basis of cardiac rapid and slow delayed rectifier potassium channels. *Cell. Physiol. Biochem.* **9:**201–216

Nerbonne, J.M. 2000. Molecular basis of functional voltage-gated $K^+$ channel diversity in the mammalian myocardium. *J. Physiol.* **525:**285–298

Pajor, A.M., Hirayama, B.A., Wright, E.M. 1992. Molecular biology approaches to comparative study of $Na^+$-glucose cotransport. *Am. J. Physiol* **263:**R489–R495

Pfaffl, M.W. 2001. A new mathematical model for relative quantification in real-time RT PCR. *Nucleic Acids Res.* **29:**e45

Pond, A.L., Nerbonne, J.M. 2001. ERG proteins and functional cardiac $I_{Kr}$ channels in rat, mouse, and human heart. *Trends Cardiovasc. Med.* **11:**286–294

Sanguinetti, M.C., Jiang, C., Curran, M.E., Keating, M.T. 1995. A mechanistic link between an inherited and an acquired cardiac arrhythmia: HERG encodes the $I_{Kr}$ potassium channel. *Cell* **81:**299–307

Sanguinetti, M.C., Jurkiewicz, N.K. 1990. Two components of cardiac delayed rectifier $K^+$ current. *J. Gen. Physiol.* **96:**195–215

Shoeb, F., Malykhina, A.P., Akbarali, H. I. 2003. Cloning and functional characterization of the smooth muscle ether-a-go-go-related gene $K^+$ channel. *J. Biol. Chem.* **278:**2503–2514

Trudeau, M.C., Warmke, J.W., Ganetzky, B., Robertson, G. 1995. HERG, a human inward rectifier in the voltage-gated potassium channel family. *Science* **269:**92–95

Tseng, G.N. 2001. $I_{Kr}$: the hERG channel. *J. Mol. Cell. Cardiol.* **33:**835–849

Warmke, J.W., Ganetzky, B. 1994. A family of potassium channel genes related to *eag* in *Drosophila* and mammals. *Proc. Natl. Acad. Sci. USA* **91:**3438–3442

Yellen, G. 2002. The voltage-gated potassium channels and their relatives. *Nature* **419:**35–42